Sensitivity Studies of Tropical Storm Genesis Using a Numerical Model

ROBERT E. TULEYA

Geophysical Fluid Dynamics Laboratory/NOAA, Princeton, New Jersey

(Manuscript received 11 April 1990, in final form 19 September 1990)

ABSTRACT

This study investigates two cases of the FGGE III-B tropical cyclone genesis study of Tuleya (1988) in more detail. These two cases occurred within a week of one another in the tropical North Atlantic in August 1979. One disturbance developed into Hurricane David, the other did not develop past the depression stage. At one point in their evolution the disturbances had quite similar values of low-level vorticity. In the developing case of Hurricane David, the disturbance propagated along in a low-level wave trough with an accompanying high wind maximum. In the nondeveloping case the initial disturbance was also embedded in a wave trough with an associated wind maximum. This low-level wave propagated westward leaving the depression in its wake. The different environmental flow was responsible for the different behavior. Synoptic and budget analyses revealed significant differences in disturbance structure and vorticity and equivalent potential temperature tendencies at the time of approximate equal strength of the two disturbances. The evolution of these two disturbances was quite robust even to reasonable increases to the initial relative humidity.

Supplementary experiments of the developing case were performed by altering the sea surface temperature and surface evaporation. It was found that the difference in storm evolution was minor in a case when climatological mean values of sea surface temperatures were specified. The climatological mean values were ~0.5 K lower than the August 1979 mean used in the control simulation. In addition, an experiment without evaporation led to a propagating easterly wave with little development. Furthermore, when the evaporation was specified to a climatological constant value, there was intensification into a weak tropical storm with a rather peculiar structure. Apparently, at least in this case, processes other than evaporation-wind feedback led to moderate storm intensification.

1. Introduction

The process by which a tropical storm is formed has been a fascinating but complicated subject for many years. Traditionally, genesis has been defined as the stage of development whereby a disturbance exceeds a low-level wind speed of gale force (~ 17 m s^{-1}) and achieves storm status according to WMO definitions. Often the terms formation and development are used for earlier and later stages of the life cycle of tropical cyclone, but at times these terms are used interchangeably (Frank 1987). Genesis has been studied by observational, theoretical, and numerical means. There have been contrasting approaches to studying this phenomenon including idealized, case study, and composite data methods. In theoretical work, both linear and finite amplitude instabilities have been investigated. Progress has been handicapped by lack of observations in the data sparse regions of formation and deficiency of physical understanding of convective and multiple scale interaction processes.

Corresponding author address: Robert E. Tuleya, Geophysical Fluid Dynamics Lab, P.O. Box 308, Princeton, NJ 08542.

Recent studies of genesis have reemphasized the important role of the finite amplitude approach whereby a preexisting disturbance of sufficient strength is a prerequisite for storm formation (Emanuel 1989). The crucial role of surface evaporation was also reemphasized (Rotunno and Emanuel 1987), while others have shown the critical influence that nonlinearity plays in storm development (e.g., Hack and Schubert 1986). Recent works have tended to downplay CISK instability (Charney and Eliassen 1964; Ooyama 1964) as a genesis mechanism because of questions concerning its linear nature and reliance on inherent convective instability.

Observational studies involving composite and climatological datasets (e.g., McBride and Zehr 1981) have, in effect, taken advantage of the finite amplitude nature of the problem by studying the different stages of development. These studies have shown the critical importance of low-level entropy and environmental winds. Recently, aircraft investigations (Middlebrooke 1988) have revealed the relatively high vorticity associated with convective core regimes in both developing and nondeveloping incipient disturbances.

Three-dimensional (3-D) numerical models have shown increasing skills in simulating genesis when starting from a preexisting finite-amplitude distur-

bance. Early simulations utilized idealized initial conditions (Tuleya and Kurihara 1981), while later experiments used the FGGE III-B dataset to demonstrate the feasibility of simulating and forecasting tropical cyclogenesis with regional (Tuleya 1988, hereafter referred to as RT) and global (Krishnamurti et al. 1989) models. Composite datasets have been recently used by Challa and Pfeffer (1990) to simulate developing and nondeveloping systems.

Unfortunately, interpretation of modeling studies often seems as difficult as the observed phenomena with developing and nondeveloping systems being surprisingly alike. One must also keep in mind the possible differences between model and reality. However, in a numerical model one can isolate different components of a process. In the present study, the results of RT will be analyzed in more detail, differentiating between a developing and nondeveloping case in section 2. Equivalent potential temperature and vorticity tendencies will be analyzed at the time of approximate equal strength of each system. The sensitivity to the initial moisture of these two case studies will also be evaluated.The model's sensitivity to sea surface temperature (SST) change from observed to climatological mean and to changes in surface evaporation will be evaluated for the developing case in section 3. The results will be summarized in section 4.

2. Contrast between observed developing and nondeveloping cases

The experiments of RT successfully simulated a developing and a nondeveloping case of tropical storm genesis during late August 1979 in the tropical North Atlantic using the FGGE III-B dataset of ECMWF. This study utilized a 3-D primitive equation, 11-level model with uniform horizontal resolution of 0.25°, and a domain size of 3°S to 27°N and 60°W to 24°W. Other simulated cases in the northwest Pacific and Indian oceans reinforce the validity of these results. A satellite composite of these two disturbances, which occurred a week apart, is shown in Fig.1. This study will utilize the findings from these two case studies as well as additional information derived from sensitivity experiments.

The experiment A25 case of Hurricane David simulated the observed development of a tropical storm with a 72-h track error of ~233 km and low-level winds exceeding 30 m s^{-1} as seen in Fig.2. The nondeveloping system observed a week prior to David was simulated in experiment A18 with the model indicating a propagating wave near Barbados at 72 h and a slowly moving depression that was initially embedded in the wave trough. Little significant increase in low-level wind speed occurred in either the wave or the residue depression despite an active convective area (Figs. 1 and 2). Another encouraging indication of the model's validity was the similarity of the 24–36 h precipitation patterns to observed cloud photos in experiment A18 (RT) and experiment A25 (Tuleya 1986). Some significant early stage differences between these two cases were shown by RT, including relatively low initial moisture and high vertical wind shear in experiment A18 compared to experiment A25. After 36 h, the disturbance of experiment A18 appeared to lose its moisture and precipitation. This corresponds roughly to the satellite photo of Fig. 1. These two cases will now be discussed in more detail.

a. Time evolution of the two cases

In the developing case of David, the disturbance occurred and intensified in deep easterlies. This led to a persistent movement westward of both the observed and simulated (experiment A25) disturbance. There was good agreement with the National Hurricane Center best track and satellite observations (Fig. 1). The intensification was consistent with little apparent shear in the vertical, adequate low-level moisture, positive low-level vorticity, and consequently high genesis potential (Gray 1979; Hebert 1978). The potential minimum central pressure based on the formulation of Emanuel (1988) was 915 mb and the genesis potential parameter based on Gray (1979) was 45 units at 12 h. Typical values of the genesis parameter for individual disturbances range from ~20 units and below for nondeveloping depressions to values > 20 units for developing depressions and ~200 units for a tropical cyclone. Figure 3 (bottom) displays the area of low-level wind greater than 10 m s^{-1} associated with the easterly wave as it moved concurrently with the deepening low-level depression center near the axis of the trough. According to Lee et al. (1986) this can be interpreted as a "wind surge," although both propagation of wind maxima and locally forced wind intensification are found in the numerical simulation of several genesis cases. One can also analyze the evolution of the equivalent potential temperature profile for a 5° × 5° area surrounding the developing system (Fig.4 upper right). Significant features include the systematic increase of θ_e in the boundary layer and decrease at the tropopause level as the system intensifies. At middle levels there was little change in the profiles after the first day. On the other hand, if one looks at an 1° × 1° area surrounding the storm (Fig. 4 lower right) the effects of cumulus convection are more apparent with a systematic heating and moistening of the middle levels as the system develops.

On the other hand, the nondeveloping case evolution is more complex. The satellite photo of Fig. 1 indicates the rather slow movement of the cloud cluster and the apparent remnant of the convective region on 21 August. On the other hand, a steady large-scale wave propagation is indicated in the observed FGGE III-B analysis and by Frank and Clark (1980). This corresponds somewhat to the evolution of the disturbance and wave in experiment A18 (Fig. 3). In the model the

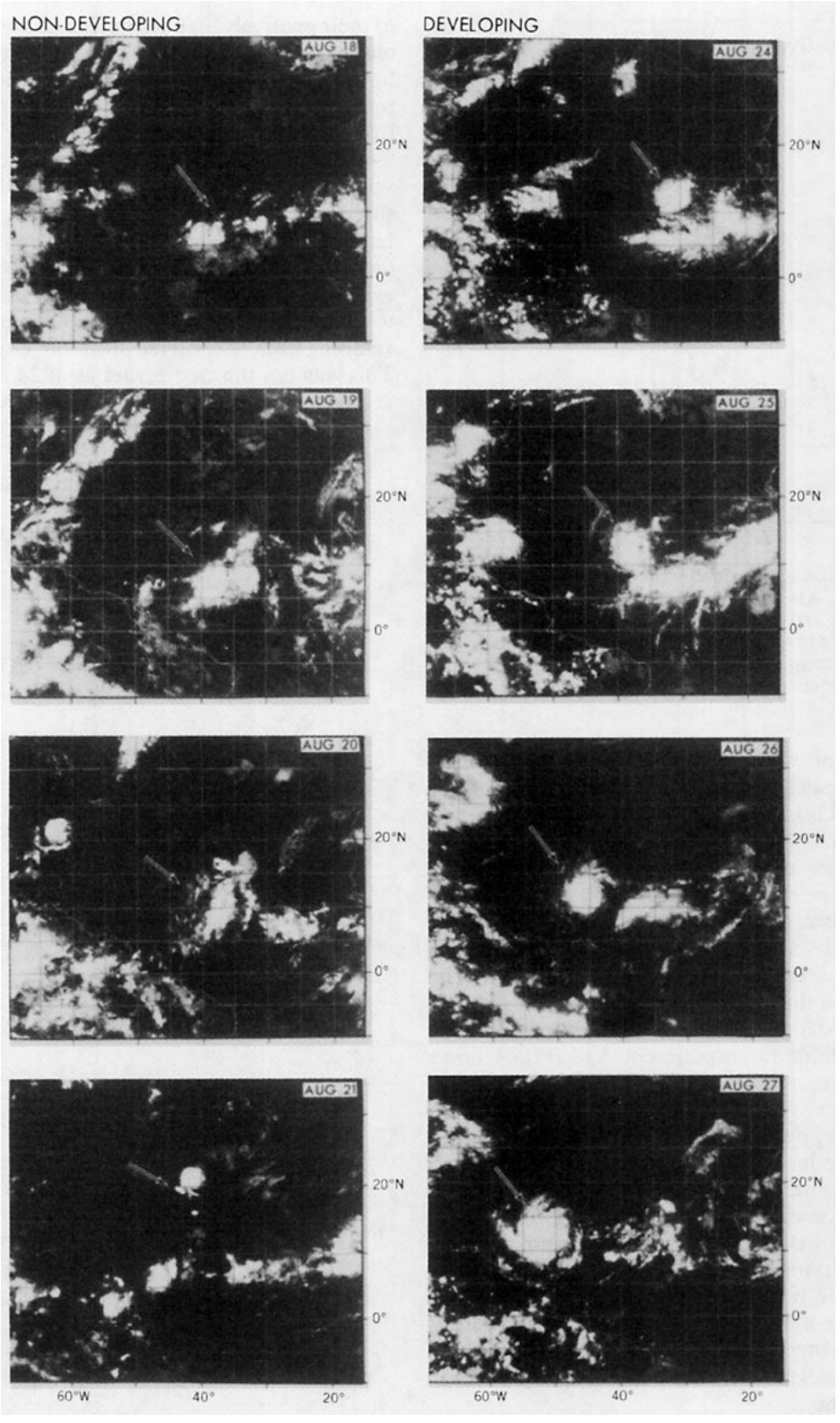

FIG. 1. Daily infrared satellite photos of a nondeveloping (left) and a developing (right, David) disturbance in the tropical North Atlantic for August 1979. The arrow denotes approximate disturbed region.

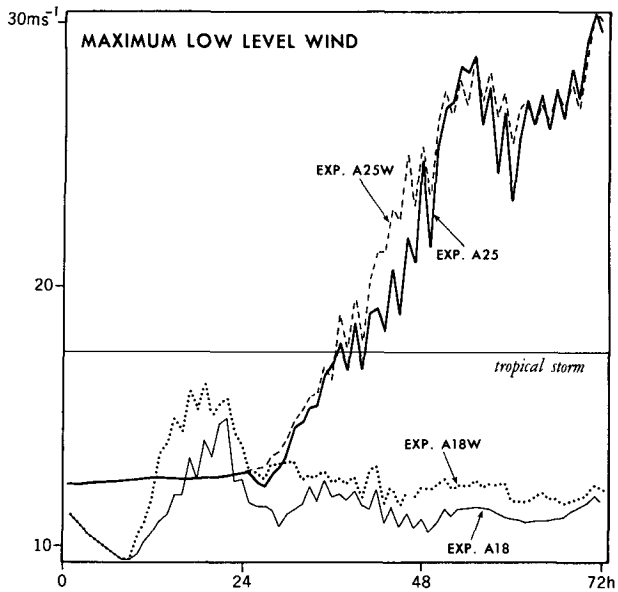

FIG. 2. The maximum low-level wind at $\sigma = 0.992$ (~68 m) for experiments A18, A18W, A25, and A25W as a function of time. Experiments A18 and A18W were for a nondeveloping case and experiments A25 and A25W for the developing case of David. The suffix "W" denotes an increase in relative humidity of 10% in the FGGE III-B initial conditions.

low-level strong wind area associated with the wave propagates westward leaving the low-level depression in its wake. This is quite different from the developing David case. It is interesting that the potential central surface pressure using the Emanuel formulation for this system is ~907 mb primarily because of the relatively low values of moisture in the environment. The Gray potential was 24 units, less than the developing case primarily because of high vertical wind shear. This suggests that in this case the environmental wind contributes to the demise of the incipient disturbance. The $5° \times 5°$ θ_e profile for experiment A18 (Fig. 4 upper left) indicates an initial increase of θ_e at low and middle levels. However, as the system decreased in intensity the values of θ_e decreased to those even below initial ones at middle levels. The middle level decrease after 24 h is even more dramatic for the $1° \times 1°$ area near the disturbance center (Fig. 4 lower left). It can be shown that this decrease is due to a combination of cooling and drying. Notice the continued increase in θ_e until after 48 h in the boundary layer. This is consistent with the hypothesis that in this case, the demise of the disturbance can be attributed to midlevel advective processes rather than direct consequences of surface influences.

b. Synoptic contrast between the two cases

To enlighten the understanding of the actual processes relevant during genesis, these two numerical simulation experiments were contrasted with the use of their relatively high resolution model data. The time chosen for analysis was 30 h because the disturbances have several similarities at that time including approximately the same low-level vorticity (Fig. 5). At this time in the nondeveloping case the low-level wind is ~4 m s^{-1} less than that of the developing case. The vorticity ($\sim 30 \times 10^{-5}$ s^{-1}) is comparable to that measured for observed developing and nondeveloping systems by aircraft penetration (Middlebrooke 1988). The developing system has more shear vorticity and little evidence of cross-equatorial southwesterlies. In contrast to the nondeveloping case, the precipitation of the developing case is centered near the depression center. This was not the case earlier as at 24 h the main convective area was to the north of the developing surface

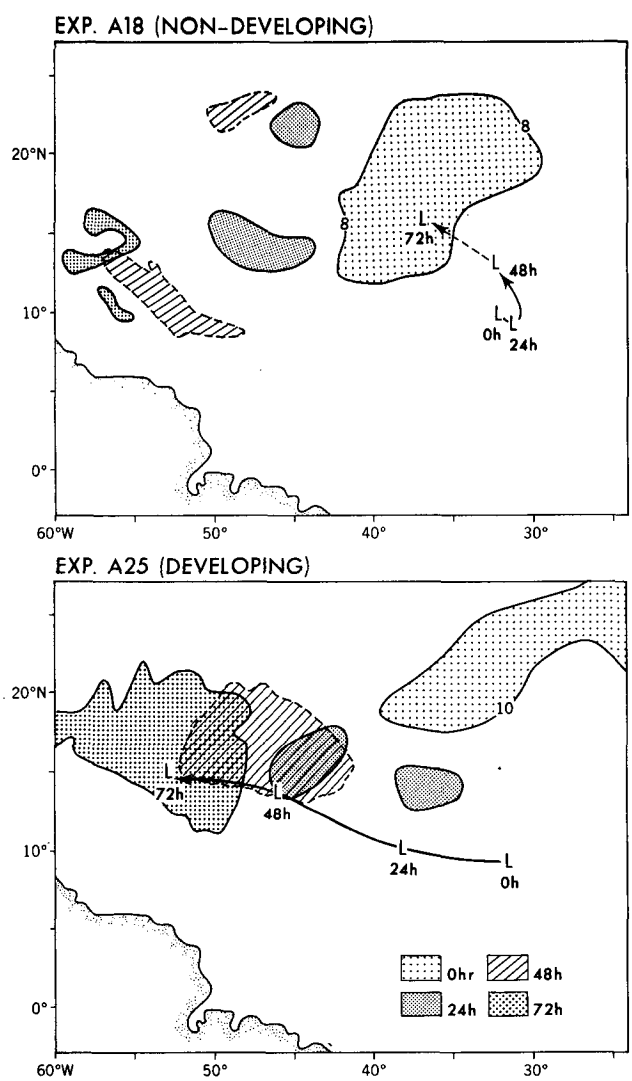

FIG. 3. Daily time history of the strong low-level wind area associated with the initial trough (shading) and low-level depression ("L") track for 18–21 August (top) and 25–28 August (bottom) 1979 for experiments A18 and A25, respectively. Areas of wind speed >8 m s^{-1} and >10 m s^{-1} are shaded in top and bottom, respectively.

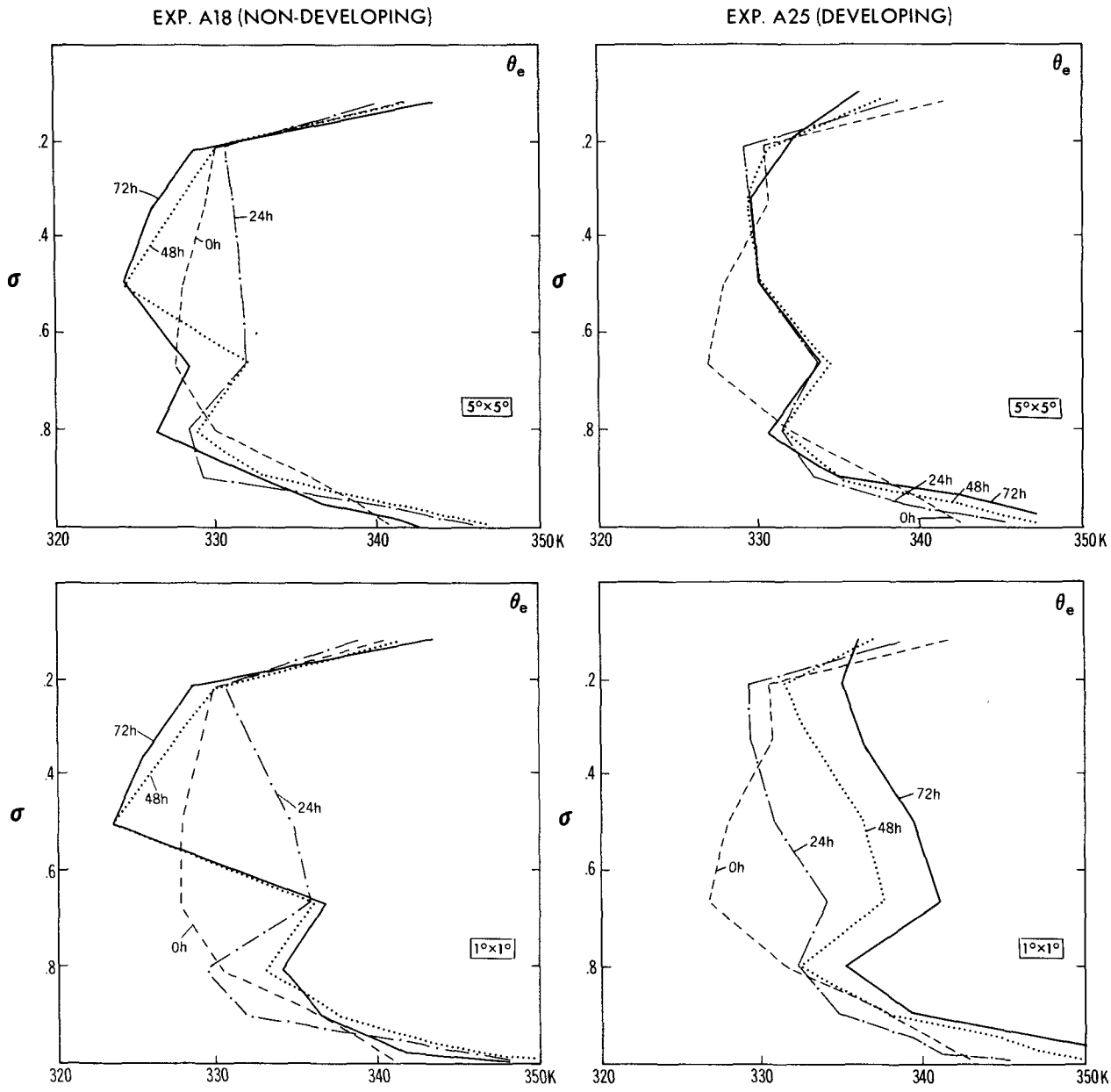

FIG. 4 Profiles of equivalent potential temperature at 24-h intervals for a 5° × 5° area surrounding the disturbance of experiment A18 (top left) and experiment A25 (top right). The bottom profile are those for experiment A18 (left) and experiment A25 (right) except for a 1° × 1° area surrounding the disturbance.

depression. Observations have often shown cloud clusters not to be aligned with the center of circulation even for developing systems (e.g., Fett 1966). This evidence suggests that net upper-level warming might not occur through convective heating alone. Indeed, in the developing case (Fig. 5, right) the upper-level warm areas are associated with both large upward motion and relatively large subsidence in a manner similar to the study of Yanai (1961). In both the developing and nondeveloping waves, broad upper-level warm areas occur to the west and ahead of these troughs. In the developing case the warm core forms on the eastern edge of this broad warm area. In the nondeveloping case, the upper-level temperature above the surface depression is generally cool. A strong correlation occurs between subsidence and warming, and upward motion and cooling (Fig. 5, left).

In the tropics, there is a delicate balance between heating and vertical motion so other terms such as horizontal advection may become important in the process of warm core formation. Although the upper-level winds are quite different from one level to the next in

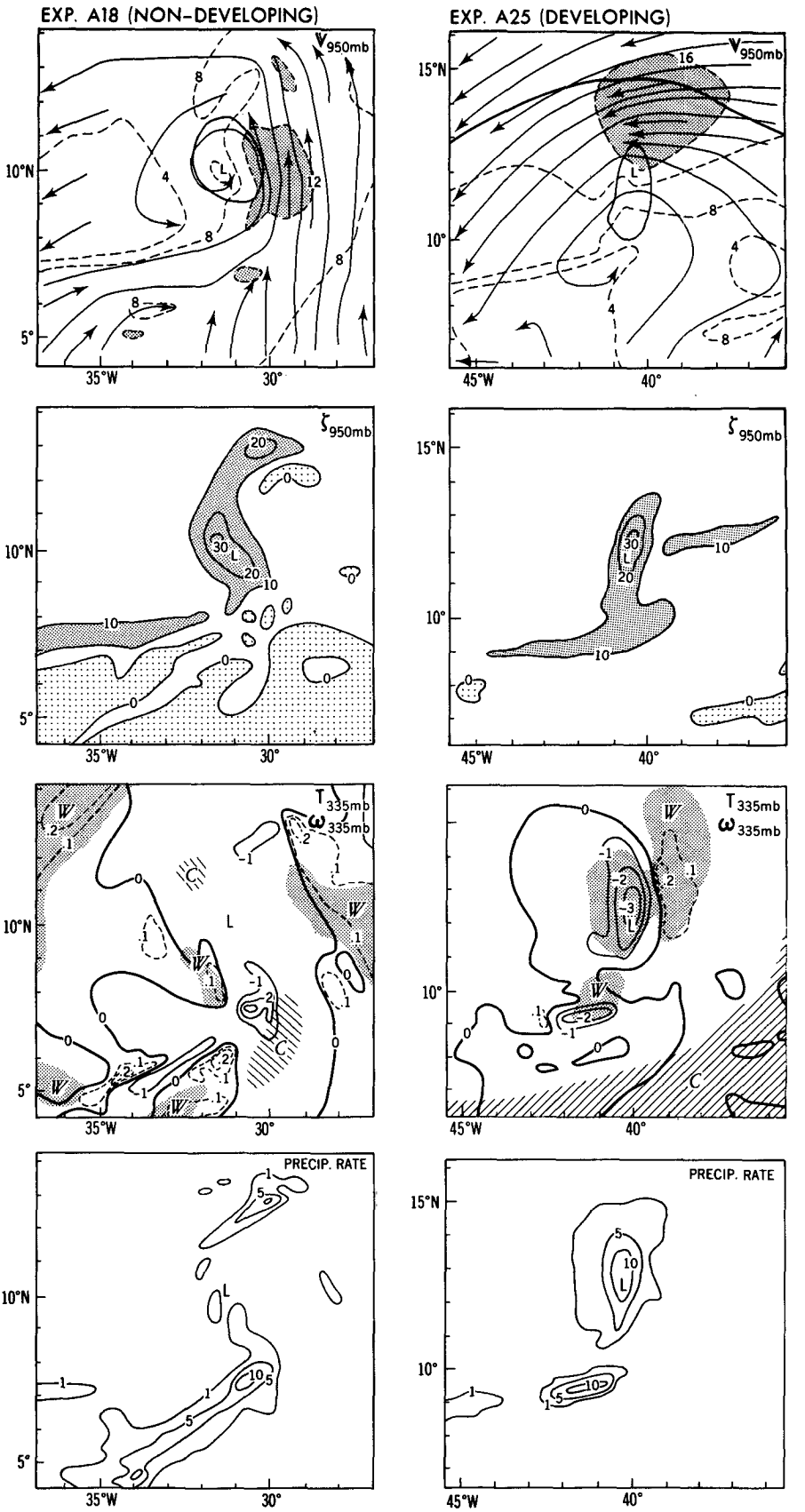

FIG. 5. Low-level wind field (m s^{-1}), low-level vorticity (10^{-5} s^{-1}), 335-mb vertical motion (10^{-2} mb s^{-1}), warm (>248 K) and cold (<247 K) temperature anomalies, and precipitation rate (mm h^{-1}) at 30 h for experiment A18 (left) and experiment A25 (right).

the nondeveloping system, an anticyclone occurs to the northeast of the surface disturbance between 100 and 300 mb. Strong southwesterlies persist aloft to the west of this anticyclone, especially at 215 mb (RT). Upper-level winds lead to ventilation or cooling above the surface disturbance which will be shown later in this section. For the developing case, significant upper-level westerlies do not penetrate the region over the low-level depression.

c. Vorticity tendency of the two cases

It is informative to look at the vorticity budget following the disturbance at 30 h for the two cases. According to Kurihara and Tuleya (1981), the rate of change of the absolute vorticity of the moving system may be written as:

$$\frac{D(\zeta+f)}{Dt} = -(\mathbf{V}-\mathbf{C})\cdot\nabla(\zeta+f) - \omega\frac{\partial\zeta}{\partial p} + (\zeta+f)\frac{\partial\omega}{\partial p} + ZD + ZE \quad (2.1)$$

where the first two terms on the right are the tendencies due to relative horizontal and vertical advection, $(\zeta+f)\partial\omega/\partial p$ is the stretching term, and ZD and ZE are the twisting and frictional terms. In (2.1), D/DT indicates the change relative to the disturbance that moves with phase velocity **C**, **V** is the horizontal wind, ω is the vertical p velocity, ∇ the horizontal gradient operator, ζ the relative vorticity, and f the Coriolis parameter. For these two particular cases, ZD and ZE were computed and found to be nearly negligible. A circular average is displayed (Fig. 6) to more adequately represent the 3-D field surrounding the depression center. Notice the similarities of both the distribution and the maximum values ($>10\times10^{-5}$ s^{-1}) of the relative vorticity in the two simulations. The maximum relative vorticity increased from $\sim3\times10^{-5}$ s^{-1} in the initial FGGE III-B fields apparently in part due to the horizontal resolution difference between the FGGE III-B grid and the present model grid. Recent aircraft measurements (Middlebrooke 1988) have shown that relative vorticity values may be greater than previously anticipated by the use of large-scale analysis or through compositing of coarse resolution datasets. Significant net positive tendencies extend through a deep layer in the developing case near the center. Each of three components play a significant role in this positive net tendency: deep stretching, even above the boundary layer; advective concentration of vorticity toward the center, an apparently highly nonlinear process (Hack and Schubert 1986); and an upward advection of low-level vorticity above the boundary layer. The horizontal advection term is quite similar in form to the net vorticity tendency for the developing case. These budget terms are quite similar to that analyzed in the idealized experiments of Kurihara and Tuleya (1981). In addition, observations indicate that a deep layer of convergence, which implies deep stretching, is required for developing systems (e.g., Gray 1979; Middlebrooke 1988).

The upper-level minimum in vorticity occurs at a lower level ($\sim$300 mb) in the nondeveloping case than in the developing case, which is consistent with the absence of a warm core near 335 mb (Fig. 5 left). If one looks at the net vorticity tendencies, one sees few significant positive values except at low levels for the nondeveloping case. At this stage for both the developing and the nondeveloping system, the eddy (relative to a circular average) flux convergence of eddy vorticity was negligible near the system center except in the boundary layer. In the outer fringes of both disturbances beyond $\sim$300 km from the center, the eddy and mean flux terms of vorticity convergence were comparable in magnitude. At an earlier stage of development for these two cases, it is uncertain whether eddy transport was significant as suggested by Challa and Pfeffer (1990).

d. Equivalent potential temperature tendency of the two cases

The equivalent potential temperature tendency equation following the disturbance was also calculated at 30 h for both developing and nondeveloping cases. The equivalent potential temperature $\theta_e \approx \theta(1 + Lr/c_pT)$, is a quasi-conservative quantity for moist processes, combining both temperature and moisture. Its distribution in the tropics, in general, and in tropical disturbed regions specifically is well known. Following Rotunno and Emanuel (1987), but taking the disturbance motion into account, the equivalent potential temperature change for the moving disturbance may be written as:

$$\frac{D\theta_e}{Dt} \approx -(\mathbf{V}-\mathbf{C})\cdot\nabla\theta_e - \omega\left(\frac{\partial\theta_e}{\partial p}\right) + \left.\frac{\partial\theta_e}{\partial t}\right]_{adj} + D\theta_e + VF\theta_e + HF\theta_e \quad (2.2)$$

where the first term on the right is the change due to relative horizontal advection, the second term is that due to resolvable scale vertical motion, $\partial\theta_e/\partial t]_{adj}$ is the change due to condensation–convection, $D\theta_e$ is the change due to radiation, and $VF\theta_e$ and $HF\theta_e$ are the effects of vertical and horizontal diffusion respectively. The circular average cross section is displayed in Fig. 7. The radiation effect, although not shown because of its small magnitude, may not be negligible in the genesis process (Kurihara and Tuleya 1981). The horizontal diffusion effect is also small, and therefore not shown in Fig. 7. As is implied in Figs. 4 and 5, a deep anomalously warm ($>$1.2 K) and moist ($>$2 g kg^{-1}) area extends above 400 mb for experiment A25. As in Yanai (1961, 1968), cool anomalies and cooling tendencies were found above the warm core at $\sim$100 mb. In the

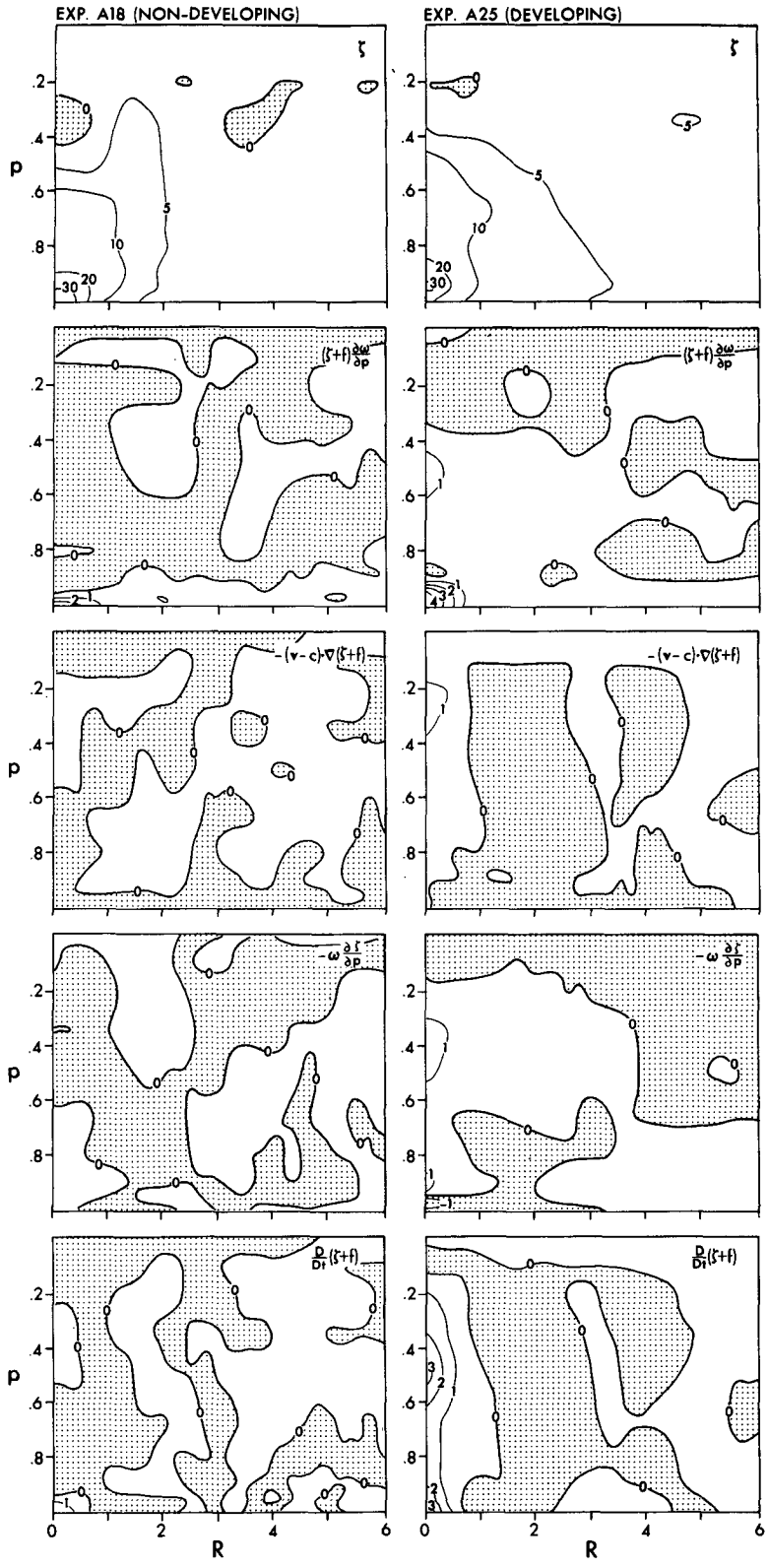

FIG. 6. Circular average of relative vorticity (top, 10^{-5} s^{-1}) and its net tendency (bottom, 10^{-8} s^{-2}) at 30 h for experiment A18 (left) and experiment A25 (right). Important terms in the relative vorticity tendency including the effects of stretching, horizontal and vertical advection are also shown. Vertical coordinate is 10^3 mb and radial distance from the center is expressed in degrees latitude.

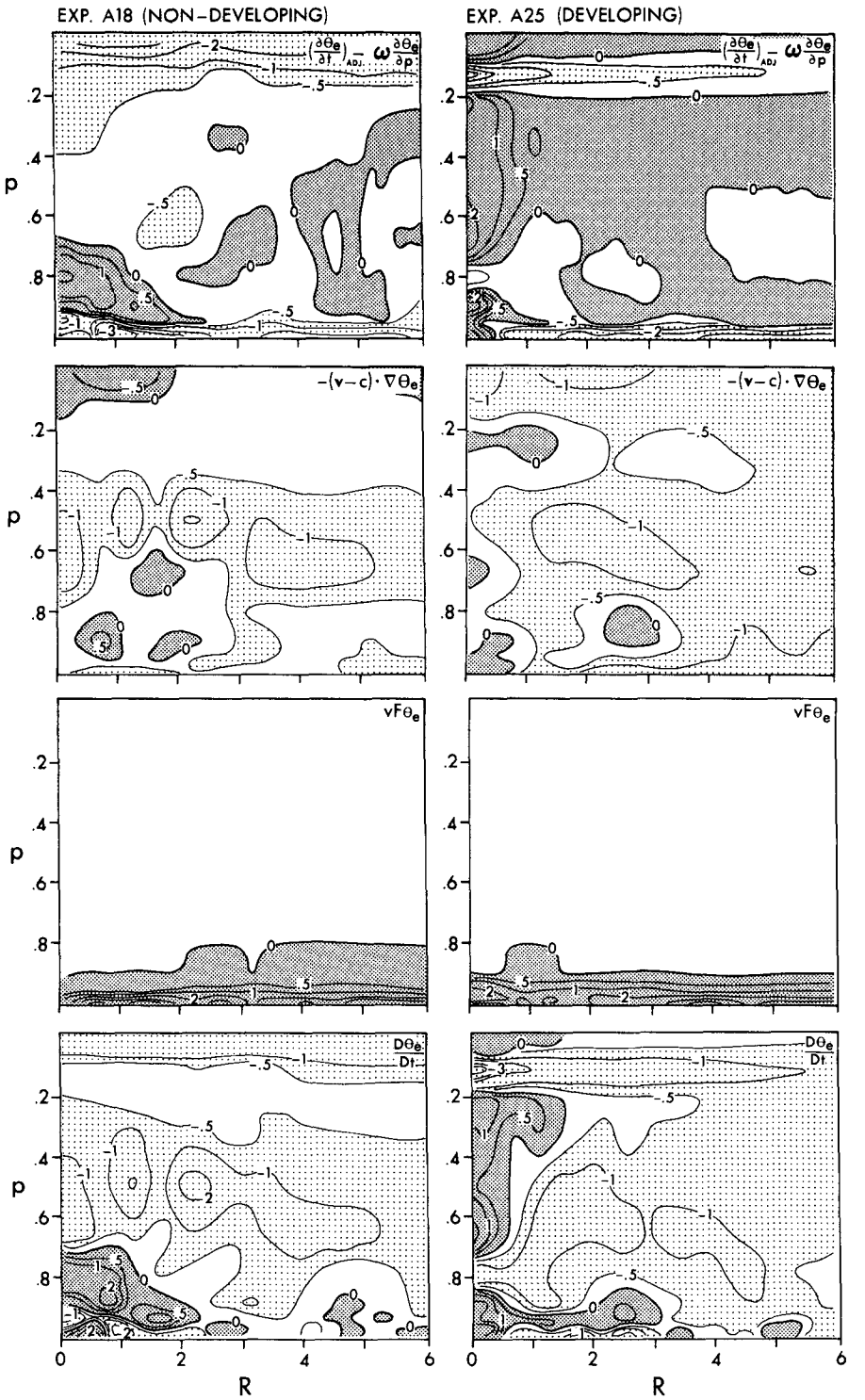

FIG. 7. Circular average of the net equivalent potential temperature tendency (bottom, 10^{-4} K s^{-1}) at 30 h for experiment A18 (left) and experiment A25 (right). Important terms in the tendency including the net effect of vertical motion and condensation, relative advection, and vertical diffusion are also shown. Radiational and horizontal diffusive tendencies are not shown. Vertical coordinate is 10^3 mb and radial distance is expressed in degrees latitude.

developing case, the net tendency of θ_e near the disturbance center displays an increase nearly throughout the troposphere. Also note the increase in boundary layer θ_e above the surface layer extending beyond 3° radially from the developing system's center. This tendency is consistent with the time evolution displayed in Fig. 4 in which θ_e increased significantly above the boundary layer near the center, and increased in the boundary layer and decreased at the tropopause in both the storm core and surrounding regions. This tendency implies consistent core moistening and upper-level heating above the storm center, where warm core formation is conducive for further intensification. The deep increase in θ_e near the center has been shown both observationally and theoretically to be consistent with a developing tropical storm. This net increase is a direct result of a small imbalance between subgrid scale convection and resolvable scale vertical motion $\{\text{i.e., } \partial\theta_e/\partial t]_{adj} - \omega(\partial\theta_e/\partial p)\}$. The relative advection, sometimes referred to as ventilation, reduces θ_e throughout most of the atmosphere, but interestingly, is negligible near the developing core region. Both the radiational and the ventilation terms act to concentrate the increase of θ_e near the center by their relative decrease of θ_e surrounding the developing disturbance core. The importance of evaporation, the surface source of $VF\theta_e$, is shown in Fig. 7. For the boundary layer as a whole, the positive tendency of $VF\theta_e$ is approximately balanced by the ventilation, resolvable-scale vertical motion and subgrid-scale convection terms. Surrounding the developing system, the net negative near-surface tendency of θ_e may lead to an increase in surface fluxes (Tuleya and Kurihara 1982) yet relatively low surface values of θ_e may retard deep convection (Emanuel 1989).

In experiment A18, however, the significant warm anomaly extends to only ~400 mb. As mentioned in section 2b, any persistent upper-level warm anomalies were apparently uncorrelated or negatively correlated to the surface disturbance. As indicated earlier, there was a dramatic decrease in middle level θ_e near the disturbance center in the nondeveloping case. The tendency budget in Fig. 7 (left) is consistent with this trend. Aloft there is a pervasive reduction of θ_e above the surface disturbance from 700 to 200 mb where one might expect warming and moistening in a growing system. This is directly attributable to the relative advection term. A significant net positive tendency is confined to below 700 mb near the center where θ_e continues to increase after 30 h. This implies that the initial demise of this system is due to middle-level advection of low θ_e air. The reduction in boundary layer θ_e occurs later.

e. Sensitivity to the initial moisture field

Two experiments, A18W and A25W, were run with identical initial conditions to experiments A18 and A25, except the relative humidity was increased everywhere by 10%. These experiments were instituted to investigate whether the main difference between experiments A18 and A25 was due to the initial moisture field (see RT, Figs. 8 and 13). This also tested the overall sensitivity of these two cases to the moisture field since it is acknowledged that the moisture field is the least reliable field in the FGGE III-B dataset especially in the data void tropical regions. As one would expect, the increased relative humidity increased the magnitude of $\partial\theta_e/\partial z$. It is interesting that with this modification a large area (15° × 15°) average θ_e profile of A18W surrounding the disturbance corresponds quite well to that of experiment A25. Despite this, however, Fig. 2 indicates that experiments A18W and A18 behaved in a quite similar manner with little evidence of a tendency for development in either case. For the two developing cases of David, little difference is indicated in the evolution of the low-level wind field.

One sees when comparing these two sensitivity experiments with their control counterparts that a temporal compensation occurs in the moisture field. Because of the increased relative humidity in the wet cases, the surface evaporation is initially retarded while the precipitation is enhanced. This effect has the impact of gradually reducing the moisture content of the wet cases toward control case values. Therefore, it is concluded that at least in these two case studies in the tropical Atlantic, the development or nondevelopment is highly controlled by the disturbance momentum field and the environmental wind field in which the respective disturbances are embedded. Significant increases in relative humidity and therefore moist static instability did not appreciably alter the overall results.

3. Impact of surface conditions on a developing case

As previously mentioned, there has been a renewed interest in surface latent heat fluxes and their relationship to genesis, especially the role of evaporation-wind feedback. Other 2-D and 3-D numerical studies (e.g., Ooyama 1969; Rosenthal 1971; Anthes and Chang 1978; Tuleya and Kurihara 1982) have stressed the importance of SST and evaporation in both formative and mature stages of tropical cyclones. This investigation will look at the sensitivity of a control case similar to experiment A25 to changes in SST, and to changes in model formulation of evaporation. These latter experiments will show the direct impact of altering the feedback of the evaporation change to the wind field.

a. Sensitivity to SST

In the control experiment, the distribution of SST was specified as the observed August mean as given by the Climate Analysis Center (CAC) for 1979. The observed SST in the tropical Atlantic averaged ~0.5 K warmer than the long term CAC August climatology. Somewhat larger anomalies (>1.0 K) occurred in the

Cape Verde region of the eastern Atlantic near the initial position of the incipient stage of David. To test the sensitivity to SST values, a supplemental experiment to the control case was integrated with identical initial conditions but with CAC climatic mean SST for August.

Little difference in the two experiments is observed (Fig. 8) with the control case being a bit more intense ($\sim$1 m s^{-1}, $\sim$1 mb). The storm position difference at 72 h is within 50 km. However, consistent with the reduced SST in the climatic case, both the precipitation and evaporation are slightly reduced. For example, the model domain average evaporation decreased from $\sim$0.35 cm day^{-1} using the FGGE year SST to $\sim$0.31 cm day^{-1} in the climatic SST. These values can be compared with those of Peixoto and Oort (1983) and McBride (1979) of $\sim$0.4 cm day^{-1} in the tropical western Atlantic in the summer. It appears that such small SST differences have little impact on this particular case. The climatic study of Shapiro (1982) indicated that SST has little predictive capacity for the typical values of interannual variability observed (<1 K) in the tropical North Atlantic.

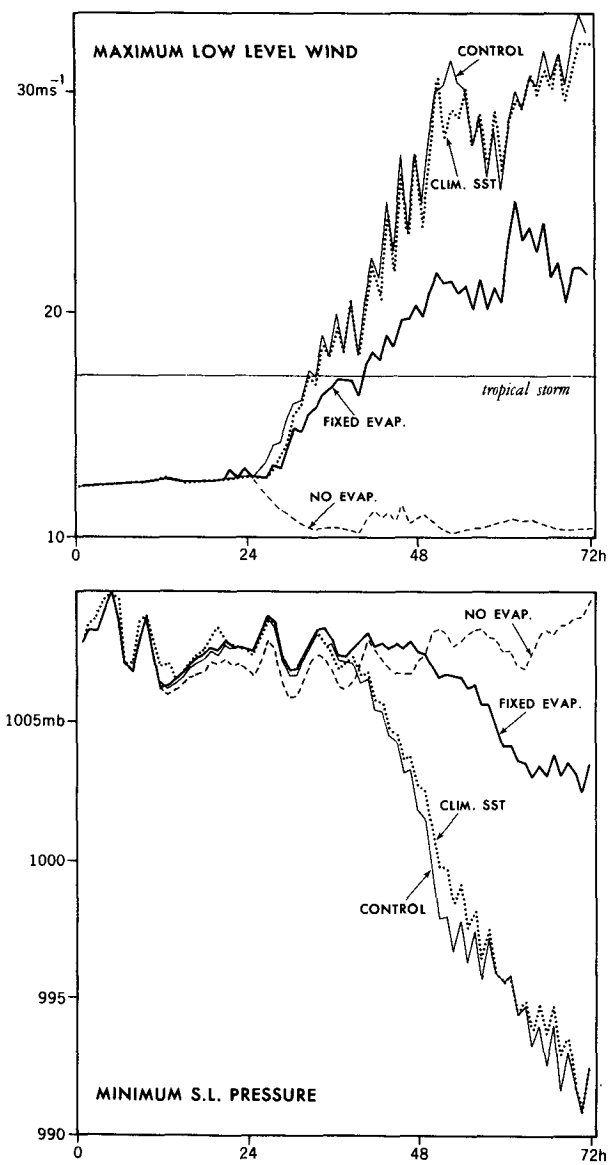

FIG. 8. The minimum sea level pressure and maximum low-level wind at σ = 0.992 ($\sim$68 m) for four sensitivity experiments starting from identical FGGE III-B conditions of 0000 UTC 25 August 1979. In the CLIM. SST case, the sea surface temperatures were set to the climatological average for August. In the NO EVAP case, evaporation from the sea surface was precluded. In the FIXED EVAP case, evaporation from the sea surface was specified everywhere to a climatological value of 0.4 cm day^{-1}.

b. Sensitivity to evaporation

Two experiments were performed to test the direct sensitivity of genesis to evaporation while eliminating any evaporation–wind feedback. One experiment was run with the evaporation set to zero, and another with the evaporation set to a climatic average of 0.4 cm day^{-1} for all sea points. In the case without evaporation, the initial wave disturbance roughly maintained its intensity as it propagated westward. Precipitation occurred near and just east of the surface trough. An upper-level warm anomaly of $\sim$1 K was observed just west of the trough. As expected, no development of the disturbance occurred (Fig. 8).

The constant evaporation case was designed to suppress the impact of the surface feedback process on tropical cyclogenesis. The scenario of the feedback is such that as evaporation increases the moist entropy of the lower atmosphere near the center of a disturbance, condensational heating and upper-level warming respond to increase the pressure gradient between the high and low entropy areas. This leads to higher low-level winds and therefore greater evaporation. Despite fixing the evaporation to a constant value in the sensitivity experiment, there was an increase of low-level winds to above tropical storm strength (Fig. 8). However, the disturbance in the fixed evaporation case intensified slowly and the pressure field failed to respond to any large extent to an increase in low-level winds and condensational heating with the central surface pressure remaining above 1000 mb. In the control experiment, the maximum evaporation associated with the disturbance increased from $\sim$1 cm day^{-1} to greater than 2 cm day^{-1} from day 2 to day 3. On the other hand, the domain-averaged precipitation in the fixed evaporation case was somewhat higher than the control case probably because the domain-averaged evaporation rate was specified somewhat larger in the constant evaporation case than that observed in the control case.

c. Synoptic view of experiment

A synoptic view of the four sensitivity experiments at the end of the integration (72 h) is presented to highlight any spatial differences in the results (Fig. 9), which

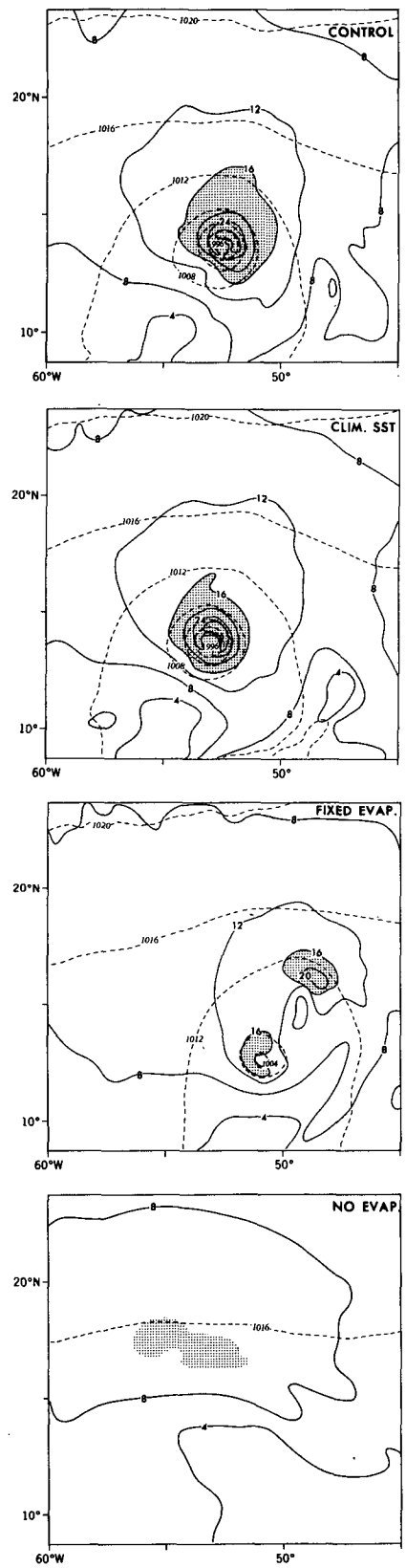

FIG. 9. The maximum low-level wind at $\sigma = 0.992$ (~68 m) (solid) and sea level pressure (dashed) for four sensitivity experiments involving surface conditions at 72 h. See Fig. 8 for more details.

may not be evident by analyzing the time history of maximum winds alone. Notice that the wind and pressure fields in the climatic SST experiment are again quite similar to those of the control case. There is some tendency for the areal extent of the 16 m s^{-1} winds to be larger in the control case where the SST is slightly higher (~0.5 K). The constant evaporation case displays a peculiar behavior at 72 h with split low-level areas of high wind. Aloft there are two warm anomalies above the associated precipitation areas. Apparently, without evaporation–wind feedback, the storm structure has less of a tendency to become concentrated into one center. This peculiar feature became more evident in the later stages of this experiment. In the case without evaporation, the wave acts similarly to a classic easterly wave with a wind maximum north along the trough axis. A weak pressure center lies nearly coincident with the actual observation of David (not shown).

4. Summary and conclusions

A case of a developing (David) and a case of a nondeveloping disturbance that occurred a week apart in the tropical Atlantic in the FGGE year (1979) have been examined more thoroughly with numerical simulations. In the developing case a more complete coupling of the low and high levels occurred due to the environmental flow and the associated weak easterly vertical shear. This enabled the low-level disturbance propagating in the low-level wave trough to move at approximately the speed of the upper-level winds. In the nondeveloping case, the incipient depression had significant low-level vorticity and precipitation. However the low-level depression and associated cloud cluster became decoupled from the wave which propagated systematically westward. The remnant depression drifted to the north and weakened. There is some support for this in observational data as well. It can be concluded that the different environmental flow was primarily responsible for this different behavior since sensitivity experiments with increased moisture failed to significantly alter these results. It should be noted that the environmental conditions that discriminated between these two cases were resolved by or evolved from the FGGE III-B analysis. It is uncertain to what extent the role of genesis processes differ from case to case and in other genesis regions where climatic conditions deviate from those of the tropical Atlantic.

The synoptic differences between the developing and nondeveloping case were examined at the stage in their life cycle when the low-level vorticity was approximately the same magnitude. Significant differences were already present aloft with warm anomalies apparently correlated with either subsidence or upward motion depending on the magnitude of other heating terms such as condensation and relative advection. The developing case had already concentrated convection near the depression, with a systematic increase in equivalent potential temperature. There was a strong

linkage between the movement of the area of low-level wind maximum near the trough and the propagation of the developing depression that was not present in the nondeveloping case. Following an initial increase, the nondeveloping case was marked by a significant decrease in equivalent potential temperature at middle levels above the incipient disturbance.

Vorticity and equivalent potential temperature tendencies following the disturbances were also examined for the two cases. In the developing case, relative horizontal advection, deep stretching, and vertical advection all combined to produce a deep positive tendency of relative vorticity. A small imbalance between subgrid-scale convection and resolvable-scale vertical motion led to warming and moistening in the core region of the developing case and therefore a significant increase in equivalent potential temperature. This tendency was further enhanced by differential effects of ventilation and radiation in the developing case. In the nondeveloping case, there was net negative vorticity tendency above the boundary layer. In addition, condensational heating and upward motion led only to low-level warming and moistening, and the ventilation effect markedly cooled and dried the incipient system aloft. The net effect was to decrease the middle-level equivalent potential temperature and thereby reduced the potential for intensification.

The sensitivity of the developing case was examined by altering the SST and the evaporation rates directly. The deviation of SST from climatic values, as typical in most years, is not large enough to significantly alter the development rate of this case. As expected, the elimination of evaporation led to nondevelopment with a resulting progressive easterly wave. If a constant, climatic value of evaporation was assumed everywhere, there was, nonetheless, development of a tropical cyclone, albeit less intense and deformed. This leads to the conclusion that air–sea feedback is not necessary for development; that other intensification processes are at work, but that evaporation–wind feedback nevertheless is quite critical for a dynamically consistent scenario in which the genesis of a compact tropical storm ensues.

Acknowledgments. The author would like to thank J. Mahlman, GFDL Director, and Y. Kurihara, project head, for their continuous support for this investigation. T. Broccoli and Y. Kurihara read an earlier version of this manuscript and provided constructive criticism. D. Golder, J. Ploshay, R. White, and M. DiPaola deserve thanks for their continuing aid in the FGGE data processing. Special credit is also given to P. Tunison, K. Raphael, J. Varanyak, and J. Conner for drafting and photographing the figures.

REFERENCES

Anthes, R. A., and S. W. Chang, 1978: Response of the hurricane boundary layer to changes of sea surface temperature in a numerical model. *J. Atmos. Sci.*, **35**, 1240–1255.

Challa, M., and R. L. Pfeffer,1990: The formation of Atlantic hurricanes from cloud clusters and depressions. *J. Atmos. Sci.*, **47**, 909–927.

Charney, J. G., and A. Eliassen, 1964: On the growth of the hurricane depression. *J. Atmos. Sci.*, **21**, 68–75.

Emanuel, K. A., 1988: Toward a general theory of hurricanes. *American Scientist*, **76**, 371–379.

——, 1989: The finite-amplitude nature of tropical cyclogenesis. *J. Atmos. Sci.*, **46**, 3431–3456.

Fett, R. W., 1966: Life cycle of tropical cyclone Judy as revealed by ESSA II and Nimbus 2. *Mon. Wea. Rev.*, **94**, 605–610.

Frank, N. L., and G. Clark, 1980: Atlantic tropical systems of 1979. *Mon. Wea. Rev.*, **108**, 966–972.

Frank, W. M., 1987: Tropical cyclone formation. *A Global View of Tropical Cyclones*, R. L. Elsberry, Ed., World Meteorological Organization, 53–90.

Gray, W. M., 1979: Hurricanes: Their formation, structure, and likely role in the tropical circulation. *Meteorology over the Tropical Oceans*, D. B. Shaw, Ed., Roy. Meteor. Soc., 155–218.

Hack, J. J., and W. H. Schubert, 1986: Nonlinear response of atmospheric vortices to heating by organized cumulus convection. *J. Atmos. Sci.*, **43**, 1559–1573.

Hebert, P. J., 1978: Intensification criteria for tropical depressions of the western North Atlantic. *Mon. Wea. Rev.*, **106**, 831–840.

Kurihara, Y., and R. E. Tuleya, 1981: A numerical simulation study on the genesis of a tropical storm. *Mon. Wea. Rev.*, **109**, 1629–1653.

Krishnamurti, T. N., D. Oosterhof and N. Digon, 1989: Hurricane prediction with a high-resolution global model. *Mon. Wea. Rev.*, **117**, 631–666.

Lee, C. S., R. Edson and W.M. Gray, 1989: Some large-scale characteristics associated with tropical cyclone development in the northern Indian Ocean during FGGE. *Mon. Wea. Rev.*, **117**, 407–426.

McBride, J. L., 1981: Observational analysis of tropical cyclone formation. Part I: Basic description of datasets. *J. Atmos. Sci.*, **38**, 1117–1131.

Middlebrooke, M. G., 1988: Investigation of tropical cyclone genesis and development using low-level aircraft flight data. *Paper No. 429, Department of Atmospheric Sci.*, Colorado State Univ.

Ooyama, K. V., 1964: A dynamic model for the study of tropical cyclone development. *Geofis. Init.*, **4**, 187–198.

——, 1969: Numerical simulation of the life cycle of tropical cyclones. *J. Atmos. Sci.*, **26**, 3–40.

Peixoto, J. P., and A. H. Oort,1983: The atmospheric branch of the hydrological cycle and climate. *Variations in the Global Water Budget*. A. Street-Perrott et al., Ed., D. Reidel Publishing Co., 5–65.

Rosenthal, S., 1971: The response of a tropical cyclone model to variations in boundary-layer parameters, initial conditions, lateral boundary conditions and domain size. *Mon. Wea. Rev.*, **99**, 767–777.

Rotunno, R., and K.A. Emanuel, 1987: An air–sea interaction theory for tropical cyclones. Part II: Evolutionary study using a nonhydrostatic axisymmetric numerical model. *J. Atmos. Sci.*, **44**, 542–561.

Shapiro, L. J., 1982: Hurricane climatic fluctuations. Part II: Relation to large-scale circulation. *Mon. Wea. Rev.*, **110**, 1014–1023.

Tuleya, R. E., 1986: The simulation of the genesis of tropical storms using the FGGE III-B dataset. *National Conf. on the Scientific Results of the First GARP Global Experiment*, Miami, American Meteorological Society, 78–80, Boston.

——, 1988: A numerical study of the genesis of tropical storms observed during the FGGE year. *Mon. Wea. Rev.*, **116**, 1188–1208.

——, and Y. Kurihara, 1981: A numerical study on the effects of environmental flow on tropical storm genesis. *Mon. Wea. Rev.*, **109**, 2487–2506.

——, and ——, 1982: A note on the sea surface temperature sensitivity of a numerical model of tropical storm genesis. *Mon. Wea. Rev.*, **110**, 2063–2069.

Yanai, M., 1961: A detailed analysis of typhoon formation. *J. Meteor. Soc. Japan*, **39**, 187–214.

——, 1968: Evolution of a tropical disturbance in the Caribbean Sea. *J. Meteor. Soc. Japan*, **46**, 86–109.